



ISSN 2278 – 0211 (Online)

Vehicle Verification Based on LG Filters

K. Deepthi Chaitanya

M.Tech (DECS), NBKRIST, Vakadu, Nellore, India

Dr. K. Nagi Reddy

Professor, Department of ECE, NBKRIST, Vakadu, Nellore, India

Abstract:

In this paper evaluation of a new descriptor based on the alternative family of log-Gabor functions for vehicle verification, as opposed to existing Gabor filter-based descriptors is proposed. These filters are theoretically superior to Gabor filters as they can better represent the frequency properties of natural images. As a second contribution, and in contrast to existing approaches, which transfer the standard configuration of filters used for other applications to the vehicle classification task, an in-depth analysis of the required filter configuration by both Gabor and log-Gabor descriptors for this particular application is performed for fair comparison. The extensive experiments conducted in this paper confirm that the proposed log-Gabor descriptor significantly outperforms the standard Gabor filter for image-based vehicle verification.

Keywords: Gabor filter, hypothesis verification, intelligent vehicles, log-Gabor filters, machine learning

1. Introduction

THE increasing interest on advanced driver assistance systems (ADAS) for the improvement of road safety has been reflected in the joint involvement of universities, research centers and car manufacturers, as well as in the deployment of national and international projects to address this issue. According to statistics, most of the accidents are caused by other cars, therefore vehicle detection arises as the key challenge for ADAS. In particular, the research on approaches based on image analysis for vehicle detection is gaining interest on account of its low cost and flexibility, and of the increased processing capabilities. A very complete survey of image-based vehicle detection can be found in [1]. Most of the reported methods address vehicle detection in two stages, namely hypothesis generation and hypothesis verification. In the former, a quick search is performed so that potential locations of the vehicles in the image are hypothesized. The search is typically based on some expected feature of vehicles, such as color [2], [3], shadow [4], [5], vertical edges [6], or motion [7]. The aim of the second stage is to verify the correctness of the vehicle candidates provided by the hypothesis generation stage. Traditionally, fixed [8] or deformable [9] models have been used for vehicle verification. However, the increase of processors speed in the last years has enabled the use of learning-based methods for real-time vehicle verification.

In particular, this is usually addressed as a two-class supervised classification problem in which a set of samples are trained in search of specific feature descriptors of the vehicle and the non vehicle classes. Some widespread descriptors include Gabor filters, principal component analysis (PCA) [10], and histograms of oriented gradients (HOG) [11], [12] In particular, Gabor filters have been broadly used for image-based vehicle verification [13]–[16]. Traditionally, a Gabor filter bank at different scales and orientations is used for feature extraction. For instance, in [15], a bank of 8 Gabor filters with 2 different wavelengths and 4 different orientations is used. In [14], Gabor filter performance is analyzed for two different configurations, using 3 scales and 5 orientations, and 4 scales and 6 orientations, respectively.

The response of each filter in the bank is typically represented by statistics such as the mean and the standard deviation, both for characterization of vehicles [13], [17] or other objects [18]–[20]. These statistics can be extracted over the whole image [18], [19] or in smaller sub windows [21].

For instance, in [14] the candidate image is divided into nine overlapping sub-windows. Alternatively, in [15], seven Hu's invariant moments [22] are derived to build the feature vector.

Other representations of texture based on Gabor filters are analyzed in [23].

Although Gabor filters have been extensively applied for a broad range of applications, they involve a number of drawbacks. First, the bandwidth of a Gabor filter is typically limited to one octave (otherwise it yields a too high DC component), thus a large number of filters is needed to obtain wide spectrum coverage. In addition, as suggested in [24], the amplitude of natural images (defined as the square root of the power spectrum) falls off in average by a factor of roughly $1/f$. This is in contrast to the properties of Gabor filters:

on the one hand, a big extent of the Gabor response concentrates on the lower frequencies, which in turn results in redundant information of the filters; on the other hand, the high frequency tail of the images is not captured.

2. LOG-GABOR Filters

As stated in Section I, the properties of Gabor filters involve two important drawbacks. On the one hand, their bandwidth must be limited in order to prevent a too high DC component. Hence, a larger number of filters is needed to cover the desired spectrum. On the other hand, their response is symmetrically distributed around the center frequency, which results in redundant information in the lower frequencies that could instead be devoted to capture the tails of images in the higher frequencies.

An alternative to the Gabor filters is the log-Gabor function introduced by Field [24]. The frequency response of log-Gabor filters in polar coordinates is given by [34]

$$LG_{m,n}(f, \theta) = \begin{cases} \exp \left\{ -\frac{(\log(f/F_m))^2}{2(\log \beta)^2} \right\} \exp \left\{ -\frac{(\theta - \theta_n)^2}{2\sigma_\theta^2} \right\} & f \neq 0 \\ 0 & f = 0. \end{cases}$$

It is also common to find in the literature their corresponding expression in the log axis [35]:

$$LG_{m,n}(\rho, \theta) = \exp \left\{ -\frac{(\rho - \rho_m)^2}{2\sigma_\rho^2} \right\} \exp \left\{ -\frac{(\theta - \theta_n)^2}{2\sigma_\theta^2} \right\}$$

Where $\rho = \log f$, $\rho_m = \log F_m$, $\sigma_\rho = \log \beta$ and $f = 0$. The parameter β determines the bandwidth of the filter. For instance, a value of $\beta = 0.75$ results in an approximate bandwidth of one octave, whereas $\beta = 0.55$ extends roughly as far as two octaves [36]. The angular bandwidth, σ_θ , is typically set to approximately 1.5 for even spectrum coverage. As can be observed in (6), log-Gabor functions are symmetrical in the log-axis instead of the linear frequency axis, which yields a more effective representation of images. Indeed, they feature a tail in the higher frequencies of the linear axis that is in line with the amplitude fall-off of natural images.

In turn, redundancy in the lower frequencies is reduced, thus achieving a more efficient coverage of the frequency spectrum. In addition, as shown in (5), the DC-component of log-Gabor filters is zero by definition, hence the bandwidth of each filter in the bank can be enlarged and the overall number of required filters can be reduced with respect to standard Gabor filters.

3. Algorithm

An alternative representation of images for vehicle classification using log-Gabor filters instead of Gabor filters is proposed and evaluated. Log-Gabor filters are designed as Gaussian functions on the log axis, which is in fact the standard method for representing the spatial frequency response of visual neurons. Their symmetry on the log axis results in a more effective representation of the uneven frequency content of the images: redundancy in lower frequencies is reduced, and the response of the filter in the linear frequency axis displays a tail in the higher frequencies that adapts the frequency fall-off of natural images. Furthermore, log-Gabor filters do not have a DC component, which allows an increase in the bandwidth, and hence fewer filters are required to cover the same spectrum. The developed algorithm flow chart is shown below figure.

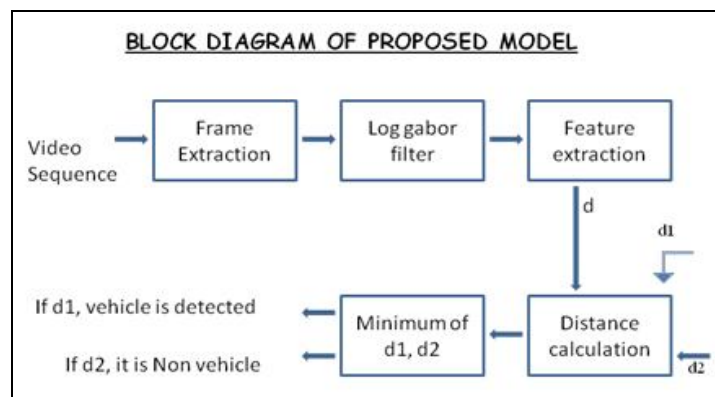


Figure 1: Block diagram of proposed model

Proposed Algorithm

Step: 1 Upload the Video sequence.

Step: 2 Extraction of frames from Video Sequence.

Step: 3 Extracted nth frames is fed to Log-Gabor Filter.

Step: 4 Features of the Filtered output is Extracted as $\mu_{m,n}$, $\sigma_{m,n}$, $\gamma_{m,n}$.

Step: 5 Vehicle parameters of (n-1)th frame is obtained as $\mu_{1m,n}$, $\sigma_{1m,n}$, $\gamma_{1m,n}$.

Step: 6 Non-Vehicle parameters of (n-1)th frame is obtained $\mu_{2m,n}$, $\sigma_{2m,n}$, $\gamma_{2m,n}$.

Step: 7 Obtained features of steps 4, 5, 6 are computed for distance calculation using $d1=(|\mu-\mu1|+|\sigma-\sigma1|+|\gamma-\gamma1|)$ and $d2=(|\mu-\mu2|+|\sigma-\sigma2|+|\gamma-\gamma2|)$

Step: 8 Minimum of the distances (d1,d2) is obtained.

case1: If d1 is minimum vehicle is detected and it is marked.

case2: If d2 is minimum it is non-vehicle and go to step3.

Figure 2: Proposed Algorithm

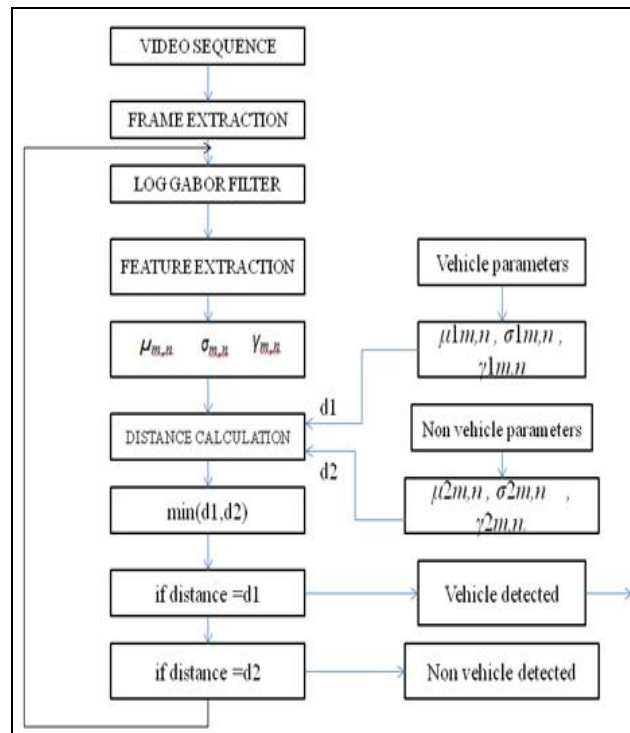


Figure 3: Flow chart of proposed algorithm

4. Experimental Results

We verified the algorithm by giving input as video sequence which contains objects like vehicles obstacles as other vehicles. algorithm works efficiently real time process because 24 frames per second video is enough for real time. We executed successfully up to 2900 frames. Some frames vehicle verified results are shown in below figure.

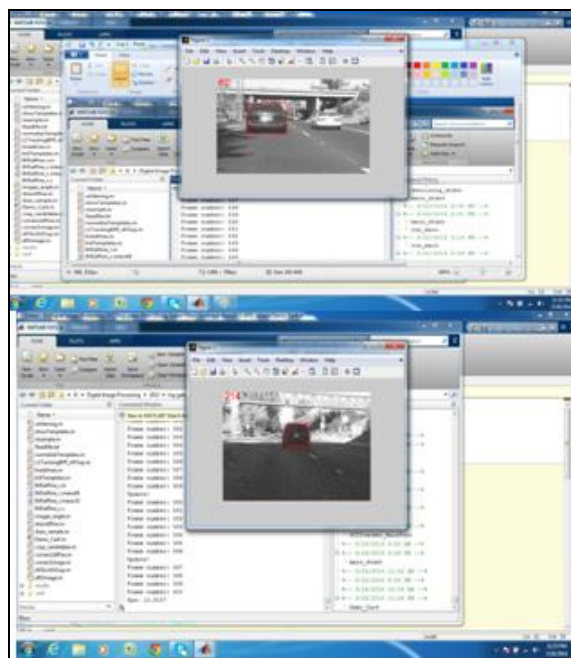


Figure 4: Experimental Results

5. Conclusion

In this study the potential of Gabor filters as descriptors for supervised vehicle classification has been assessed. First, the impact of the different design parameters of the Gabor-based descriptor has been evaluated in the field of vehicle imaging, yielding valuable conclusions. For instance, the optimal minimum wavelength of the filter bank, $\lambda(m) 0$, is proven to be dependent on the pose of the vehicles, and in particular, to increase with the relative distance to them. Therefore, the descriptor has been designed with an adaptable $\lambda(m) 0$, rendering a significant increase in performance with respect to a generic descriptor.

Most importantly, in contrast to typical approaches using Gabor filter banks, a new descriptor based on log-Gabor functions has been proposed. These functions have better theoretical properties than traditional Gabor filters for natural image representation, but had not been previously used for vehicle verification. The extensive experiments enclosed in this paper confirm the theoretical superiority of these filters over Gabor filters in this field. In particular, log-Gabor filter banks are proven to yield better results than Gabor filter banks using the same number of filters due to their more effective coverage of the spectrum, and to scale better as the number of filters decreases.

6. References

1. Z. Sun, G. Bebis, and R. Miller, "On-road vehicle detection: A review," *IEEE Trans. Pattern Anal. Mach. Intell.*, vol. 28, no. 5, pp. 694–711, May 2006.
2. C. Rotaru, T. Graf, and J. Zhang, "Color image segmentation in HIS space for automotive applications," *J. Real-Time Image Process.*, vol. 3, no. 4, pp. 311–322, Dec. 2008.
3. L.-W. Tsai, J.-W. Hsieh, and K.-C. Fan, "Vehicle detection using normalized color and edge map," *IEEE Trans. Image Process.*, vol. 16, no. 3, pp. 850–864, Mar. 2007.
4. C. Hoffmann, "Fusing multiple 2D visual features for vehicle detection," in *Proc. IEEE Intell. Veh. Symp.*, 2006, pp. 406–411.
5. J. Hwang, K. Huh, and D. Lee, "Vision-based vehicle detection and tracking algorithm design," *Opt. Eng.*, vol. 48, no. 12, pp. 127201-1–127201-12, Dec. 2009.
6. T. Wang, N. Zheng, J. Xin, and Z. Ma, "Integrating millimeter wave radar with a monocular vision sensor for on-road obstacle detection applications," *Sensors*, vol. 11, no. 9, pp. 8992–9008, Sep. 2011.
7. K. Yamaguchi, A. Watanabe, and T. Naito, "Road region estimation using a sequence of monocular images," in *Proc. 19th Int. Conf. Pattern Recognit.*, 2008, pp. 1–4.
8. J. Lou, T. Tan, W. Hu, H. Yang, and S. J. Maybank, "3-D modelbased vehicle tracking," *IEEE Trans. Image Process.*, vol. 14, no. 10, pp. 1561–1569, Oct. 2005.
9. Z. Zhang, T. Tan, K. Huang, and Y. Wang, "Three-dimensional deformable-model-based localization and recognition of road vehicles," *IEEE Trans. Image Process.*, vol. 21, no. 1, pp. 1–13, Jan. 2012.
10. J. Zhou, D. Gao, and D. Zhang, "Moving vehicle detection for automatic traffic monitoring," *IEEE Trans. Veh. Tech.*, vol. 56, no. 1, pp. 51–59, Jan. 2007.
11. T. Gandhi and M. M. Trivedi, "Video based surround vehicle detection, classification and logging from moving platforms: Issues and approaches," in *Proc. IEEE Intell. Veh. Symp.*, Jun. 2007, pp. 1067–1071.

12. N. Dalal and B. Triggs, "Histograms of oriented gradients for human detection," in Proc. IEEE Comput. Soc. Conf. Comput. Vis. Pattern Recognit., vol. 1. Jun. 2005, pp. 886–893.
13. Z. Sun, G. Bebis, and R. Miller, "On-road vehicle detection using Gabor filters and support vector machines," in Proc. 14th Int. Conf. Digit. Signal Process., vol. 2. 2002, pp. 1019–1022.
14. Z. Sun, G. Bebis, and R. Miller, "Monocular precrash vehicle detection: Features and classifiers," IEEE Trans. Image Process., vol. 15, no. 7, pp. 2019–2034, Jul. 2006.
15. P. Dalka and A. Czyzewski, "Vehicle classification based on soft computing algorithms," in LNCS, vol. 6086. Jun. 2010, pp. 70–79.
16. Y. Du and Y. Feng, "Vehicle detection from video sequence based on Gabor filter," in Proc. Int. Conf. Electron. Meas. Instrum., Aug. 2009, pp. 375–379.
17. H. Cheng, N. Zheng, and C. Sun, "Boosted Gabor features applied to vehicle detection," in Proc. 18th Int. Conf. Pattern Recognit., 2006, pp. 662–666.
18. J. Han and K.-K. Ma, "Rotation-invariant and scale-invariant Gabor features for texture image retrieval," Image Vis. Comput., vol. 25, no. 9, pp. 1474–1481, Sep. 2007.
19. B. S. Manjunath and W. Y. Ma, "Texture features for browsing and retrieval of image data," IEEE Trans. Pattern Anal. Mach. Intell., vol. 18, no. 8, pp. 837–842, Aug. 1996.
20. J. Melendez, M. Garcia, and D. Puig, "Efficient distance-based per-pixel texture classification with Gabor wavelet filters," Pattern Anal. Appl., vol. 11, nos. 3–4, pp. 365–372, Sep. 2008.
21. H. G. Jung, Y. H. Lee, P. J. Yoon, I. Y. Hwang, and J. Kim, "Sensor fusion based obstacle detection/classification for active pedestrian protection system," in Proc. 2nd Int. Conf. Adv. Vis. Comput., 2006, pp. 294–305.
22. J. Flusser and T. Suk, "Rotation moment invariants for recognition of symmetric objects," IEEE Trans. Image Process., vol. 15, no. 12, pp. 3784–3789, Dec. 2006.
23. S. E. Grigorescu, N. Petkov, and P. Kruizinga, "Comparison of texture features based on Gabor filters," IEEE Trans. Image Process., vol. 11, no. 10, pp. 1160–1167, Oct. 2002.
24. D. J. Field, "Relations between the statistics of natural images and the response properties of cortical cells," J. Opt. Soc. Amer. A, vol. 4, no. 12, pp. 2379–2394, Dec. 1987.
25. J. G. Daugman, "Uncertainty relation for resolution in space, spatial frequency, and orientation optimized by two-dimensional visual cortical filters," J. Opt. Soc. Amer. A, vol. 2, no. 7, pp. 1160–1169, Jun. 1985.
26. S. Fischer, G. Cristobal, and R. Redondo, "Sparse over complete Gabor wavelet representation based on local competitions," IEEE Trans. Image Process., vol. 15, no. 12, pp. 3784–3789, Feb. 2006.
27. T. P. Weldon, W. E. Higgins, and D. F. Dunn, "Gabor filter design for multiple texture segmentation," Opt. Eng., vol. 35, no. 10, pp. 2852–2863, 1996.
28. P. Kruizinga and N. Petkov, "Nonlinear operator for oriented texture," IEEE Trans. Image Process., vol. 8, no. 10, pp. 1395–1407, Oct. 1999.
29. X. W. Chen, X. Zeng, and D. V. Alphen, "Multi-class feature selection for texture classification," Pattern Recognit. Lett., vol. 27, no. 14, pp. 1685–1691, Oct. 2006.
30. R. Manthalkar, P. K. Biswas, and B. N. Chatterji, "Rotation invariant texture classification using even symmetric Gabor filters," Pattern Recognit. Lett., vol. 24, no. 12, pp. 2061–2068, Aug. 2003.
31. L. Cai, C. Ge, Y.-M. Zhao, and X. Yang, "Fast tracking of object contour based on color and texture," Int. J. Pattern Recognit. Artif. Intell., vol. 23, no. 7, pp. 1421–1438, 2009.
32. Z. Sun, G. Bebis, and R. Miller, "On-road vehicle detection using evolutionary Gabor filter optimization," IEEE Trans. Intell. Transp. Syst., vol. 6, no. 2, pp. 125–137, Jun. 2005.
33. J. Movellan, "Tutorial on Gabor Filters," MPLab Tutorials, UCSD MPLab, Tech. Rep., 2005.
34. M. Nixon and A. Aguado, Feature Extraction and Image Processing, 2nd ed. New York, USA: Elsevier, 2008.
35. S. Fischer, F. Šroubek, L. Perrinet, R. Redondo, and G. Cristóbal, "Selfinvertible 2D log-Gabor wavelets," Int. J. Comput. Vis., vol. 75, no. 2, pp. 231–246, Nov. 2007.
36. P. Kovese, "Image features from phase congruency," Videre, J. Comput. Vis. Res., vol. 1, no. 3, pp. 1–26, 1999.
37. GTI Vehicle Image Database. (2011) [Online]. Available: <http://www.gti.ssr.upm.es/data/>
38. S. Rüping, "mySVM-Manual," Dept. Lehrstuhl Informatik, Univ. Dortmund, Dortmund, Germany, Tech. Rep., 2000